Project 2 - Bones

Segmentation and analysis of pelvic bone in CT images

3D Image Reconstruction and Analysis in Medicine

Authors: Federica Aresu & Blanca Cabrera Gil

ABSTRACT

Pelvic bone segmentation and pubic symphysis localization are key steps for hip surgery planning. Along this line, the steps to perform multi-atlas-based segmentation to obtain the segmentation of hip bones as well as image classification are described. Affine linear registration and b-splines Free Form Deformation are used as registration methods. K-Nearest Neighbor is selected as classifier to detect the location of pubic symphysis. Accuracy of an average of 0.5 Dice Coefficient and Hausdorff Distances in range of 20-60 were obtained. These results assess the importance of the quality of atlases as prior knowledge and the registration optimization.

1. Introduction

Pelvic bone segmentation is one of the main tasks to perform hip surgery planning. Planning is key to help the surgeon visualize and prepare the operation procedure by reviewing the clinical and radiographic findings [1].

The main goal of this project is to segment the pelvic bones, femurs and the sacrum of the common images (fixed images) from 3D CT image datasets. To do so, manual segmentation of the group images was firstly implemented on the right and left femurs and hip bones as well as sacrum. Secondly, the group images were registered to the common images (ground truth) and the transformation parameter maps were extracted. Then, the obtained deformation field was applied to the manually segmented group masks. After performing multi atlas-based segmentation to the common images, the accuracy of the results was assessed. Finally, a K-Nearest Neighbor classifier has been implemented in order to localize the slices of the images which contained the pubic symphysis.

This project is divided in four main sections: *Theoretical Background*, where the basic theory of the methods used along this work is explained; *Methods and Experiments,* for which the workflow of this project is presented in more detail, following a presentation of experimental layout; *Results and Discussion,* the obtained results are presented and discussed; whereas, in the *Conclusions* are stated the overall lessons learned during the project.

2. Theoretical Background

Image segmentation is the process of dividing an image into multiple segments. Its main purpose is to locate image feature boundaries [2]. In medical image analysis, image segmentation is the main task in many medical processes such as radiation therapy and surgery planning, automatic labelling of anatomical structures, morphological and morphometrical studies and neuroimaging among others.

Atlas-based segmentation is one of the most widely used segmentation methods in medical imaging. It consists in the application of prior knowledge from a reference image (atlas) to perform the segmentation task [3].

This method can have different sources of error including registration error, the possibility that the atlas used is not anatomically representative for the specific segmentation task or the existence of labelling errors in the atlas, which cannot be solved by means of registration. This errors can be overcomed by the usage of a Multi-atlas Segmentation approach. The main benefit of using this method is that the effect of errors associated to individual images can be reduced by the combination of information [4].

Atlas-based segmentation is the result of registering the atlas images to match the image of interest. Image registration is the procedure of inferring spatial and/or temporal correspondences between image data and/or models. In this process, there are two main actors, a reference image (fixed) and the image to register (moving). The main goal of this operation is to minimize a cost function, which measures the dispairment between the two images. The optimal values that minimizes the cost are found thanks to the usage of an optimizer. Finally, a transformation is applied by means of the interpolator, which estimates the continuous values of the discrete moving image.

The accuracy of the registration can be estimated using similarity coefficients like Dice and Jaccard. The previous, measure the ratio of shared pixels between two images. On the other hand, distance measures can also be used like Hausdorff and Procrustes.

After the processing of an image, the next step is to analyse it. Image classification plays a key role in image analysis. It consist in the labelling of images into one of the predefined categories. As one of the main tasks within the field of computer vision, many techniques have been developed like artificial neural networks (ANN), Decision Tree (DT) and Support Vector Machine (SVM) [5]. In this work a K-Nearest Neighbors approach is used. This is a supervised machine learning algorithm used to solve regression as well as classification problems. This algorithm performs classification assuming similarity in proximity [6].

3. Methods and Experiments

The first step of the project was to manually segment the group images by using the MiaLab tool. The key point of this step was to have knowledge of which label belonged to each segmented bone as it will be needed in further steps.

For the subsequent steps Python was used as programming language, and Jupyter Notebook was used as work environment. In order to perform image registration, Simple Elastix was used as medical image registration library [7]. SimpleITK was proven to be very useful when dealing with image operations.

A multi-resolution approach has been used to perform the registration task between group and common images. Specifically, it has been necessary to apply affine registration as a linear method. Successively, a b-spline Free Form deformation method has been applied as non-linear registration. Along the whole process, the information of the common images (origin and pixel distance) have been applied to the group images and their respective masks. To ensure that the obtained registered masks contained integer values corresponding to the mask values, a nearest neighbor interpolation was used as resampler. This method uses the value of nearby translated pixel values to obtain the output pixel values [8].
The estimation of the transformation map was operated using *ElastixImageFilter*. Afterwards, the transformation was applied using *TransformixImageFilter* on the corresponding group mask. Once all group masks were registered, majority voting was applied to obtain one mask, being the combination of the three different atlases. This procedure consists on performing a pixel-wise voting between the registered masks [9]. Majority vote was applied for each bone mask separately. Closing morphology operation has also been implemented to fill the holes of the majority voted masks. This procedure includes dilation and erosion subsequently. This last procedure has been necessary in order to sort the misclassified pixels within the masks.
As last step of our project, the accuracy assessment was performed by using the Dice Coefficient, also called Sørensen's formula. Its equation can be found in *Equation 1*, where X and Y are the number of elements in each datasets [10]. Also, Hausdorff distance was used as accuracy indicator. This metric measures how far two datasets are in the same metric space from each other [11]. Its equation can be found in *Equation 2*.

$$\frac{2 \cdot |X \cap Y|}{|X| + |Y|}$$

Equation 1 *Dice coefficient.*

$$d_H = max\{d(X, Y),\ d(Y, x)\}$$

Equation 2 *Hausdorff distance.*

The goal of our study was to get closer to the maximum value reachable from the Dice coefficient which is equal to 1.0, as well as the minimum distance calculated with the Hausdorff distance measurement.
Finally, image classification was performed using SimpleITK implementation of K-Nearest Neighbors algorithm. As the image database contained a lot of non-relevant information, the images were subsampled down to a size of 128x128. A boundary of 20 neighbors was implemented, as well as a weighting of the neighbors corresponding to the inverse of the distance.

4. Results and Discussion

In the following section the obtained results after performing atlas-based segmentation and image classification of pubic symphysis are going to be discussed.

a. Atlas-based segmentation

The accuracy of the registration methods has been assessed by calculating the similarity between the ground truth and the obtained segmentations by means of Dice coefficient. Also the Hausdorff distance has been calculated. The results obtained can be found *Tables 1, 2* and *3*. *Figure 1* presents a visual example of the obtained masks for right and left femur, right and left hip bone and sacrum for common image 40.
The Dice coefficient obtained for the different bones is on an average of 0.5 and the Hausdorff distance have values which vary within a range of 20-60. These results are not fully satisfactory. They indicate that during the process of performing segmentation, registration and majority voting some errors have been carried and majority voting was not able to overcome them. Two possible solutions to consider in the future would be to perform more accurate initial segmentations of the group images and/or perform longer multi-resolution registrations with more optimized parameters.

Common image 40

Metric	**Right Femur**	**Right Hip**	**Sacrum**	**Left Hip**	**Left Femur**
Dice	0.62	0.59	0.19	0.54	0.53
Hausdorff	27.00	34.64	93.73	40.90	41.68

Table 1 *Accuracy results obtained for common image 40*

Common image 41

Metric	**Right Femur**	**Right Hip**	**Sacrum**	**Left Hip**	**Left Femur**
Dice	0.54	0.50	0.26	0.34	0.35
Hausdorff	27.95	45.18	55.67	54.82	45.28

Table 2 *Accuracy results obtained for common image 41*

Common image 42

Metric	**Right Femur**	**Right Hip**	**Sacrum**	**Left Hip**	**Left Femur**
Dice	0.42	0.35	0.39	0.61	0.59
Hausdorff	42.59	63.71	59.82	29.09	27.93

Table 3 *Accuracy results obtained for common image 42*

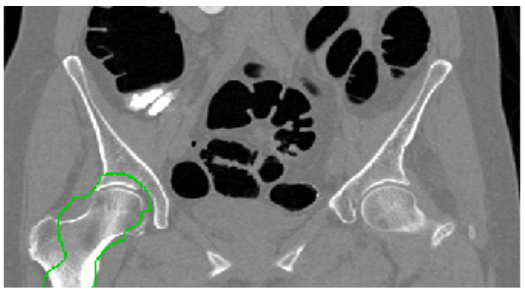

a. *Right femur segmentation*

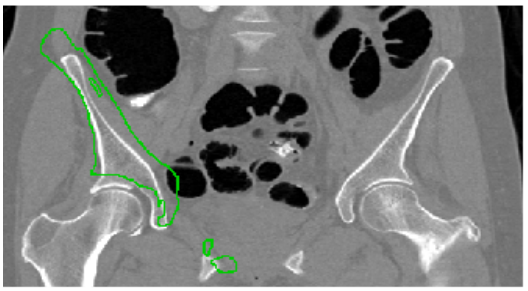

b. *Right hip bone segmentation*

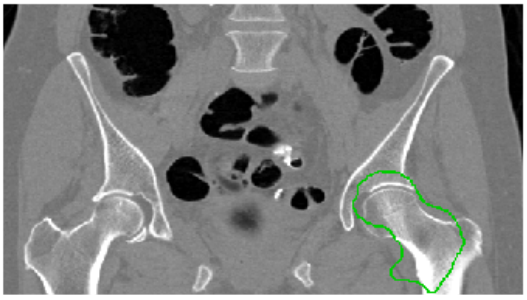

c. *Left femur segmentation*

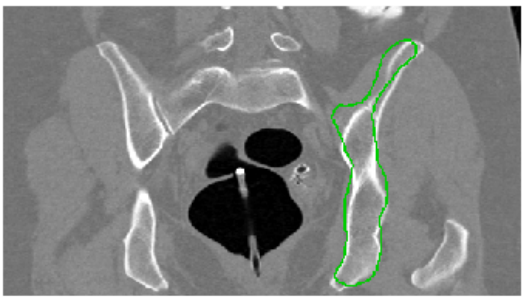

d. *Left hip bone segmentation*

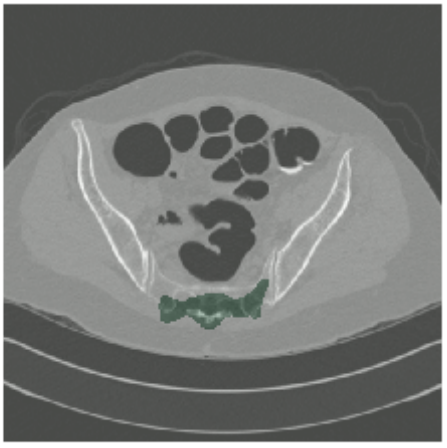

e. *Sacrum segmentation*

Figure 1 *Segmentation Results for common image 40*

b. Classifier

A K-Nearest Neighbor classifier has been implemented to perform the task of image classification. After training on downsampled images (128x128), an overall test accuracy of 84,39% was achieved. The slice with the highest probability of containing the pubic symphysis is presented in *Figure 2*.

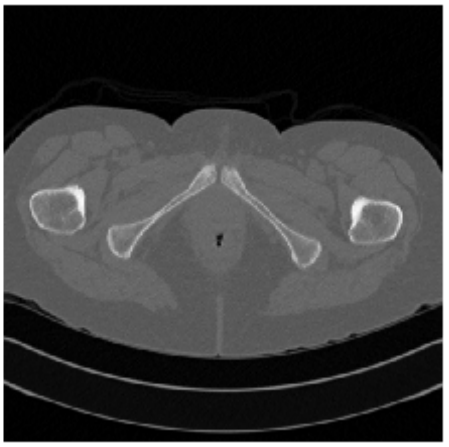

Figure 2 *Slice with the highest probability of containing the pubic symphysis.*

5. Conclusions

After analyzing the obtained results for the performed multi atlas-based segmentation and image classification the lessons learned are stated in this section. In order to obtain better performance during registration and afterwards classification of images, it is necessary to pay appropriate attention to the initial manual segmentations which will determine the following steps results. An appropriate number of iterations helps during registration process of the moving images. Non-linear registration methods as free form deformation, following linear methods are fundamental during these tasks to reduce the computational time and cost. In our mono-modality acquired images (CT), affine registration resulted the most suitable registration method among all linear registration methods available. Post-processing of the atlas-segmented mask is necessary to remove noise pixels as well to fill the holes obtained within the masks. Finally, the amount of data and the ressources is a clear determinant of the methodology for the project. Many determinants as image size, RAM capacity and GPU availability were key when trying to implement Deep Learning methods, perform image registration or just implement algorithms without an efficient memory management.

6. References

[1] Della Valle, A., Padgett, D. and Salvati, E. (2005). Preoperative planning for primary total hip arthroplasty. *J Am Acad Orthop Surg*, [online] 13(7), pp.455-62. Available at: https://www.ncbi.nlm.nih.gov/pubmed/16272270 [Accessed 24 May 2019].

[2] Tan, Y. (2016). *GPU-based parallel implementation of swarm intelligence algorithms*. Amsterdam: Morgan Kaufmann.

[3] Bach Cuadra M., Duay V., Thiran JP. (2015) Atlas-based Segmentation. In: Paragios N., Duncan J., Ayache N. (eds) Handbook of Biomedical Imaging. Springer, Boston, MA.

[4] Aljabar, P., Heckemann, R., Hammers, A., Hajnal, J. and Rueckert, D. (2009). Multi-atlas based segmentation of brain images: Atlas selection and its effect on accuracy. *NeuroImage*, [online] 46(3), pp.726-738. Available at: http://www.sciencedirect.com/science/article/pii/S1053811909001554 [Accessed 24 May 2019].

[5] Kamavisdar, P., Saluja, S. and Agrawal, S. (2013). A Survey on Image Classification Approaches and Techniques. *International Journal of Advanced Research in Computer and Communication Engineering*, [online] 2(1). Available at: https://pdfs.semanticscholar.org/9509/c435260fce9dbceaf44b52791ac8fc5343bf.pdf [Accessed 23 May 2019].

[6] Harrison, O. (2018). *Machine Learning Basics with the K-Nearest Neighbors Algorithm*. [online] Towards Data Science. Available at: https://towardsdatascience.com/machine-learning-basics-with-the-k-nearest-neighbors-algorithm-6a6e71d01761 [Accessed 25 May 2019].

[7] SimpleElastix (2018). *SimpleElastix Documentation*. [online] Available at: https://buildmedia.readthedocs.org/media/pdf/simpleelastix/latest/simpleelastix.pdf [Accessed 23 May 2019].

[8] Se.mathworks.com. (2019). *Nearest Neighbor, Bilinear, and Bicubic Interpolation Methods- MATLAB & Simulink- MathWorks Nordic*. [online] Available at: https://se.mathworks.com/help/vision/ug/interpolation-methods.html [Accessed 24 May 2019].

[9] Itk.org. (2019). *SimpleITK: itk::simple::LabelVotingImageFilter Class Reference*. [online] Available at: https://itk.org/SimpleITKDoxygen/html/classitk_1_1simple_1_1LabelVotingImageFilter.html [Accessed 23 May 2019].

[10] Dice, L. (1945). Measures of the Amount of Ecologic Association Between Species. *Ecology*, 26(3), pp.297-302.

[11] Henrikson, J. (1999). Completeness and Total Boundedness of the Hausdorff Metric. *MIT Undergraduate Journal of Mathematics*, pp.69–80.